

A New Readout Method for a High Sensitivity Capacitance Sensor Based on the Weakly Coupled Resonators [†]

Vinayak Pachkawade

University of Liege, 4000 Liège, Belgium; vpachkawade@uliege.be

[†] Presented at the 7th Electronic Conference on Sensors and Applications, 15–30 November 2020; Available online: <https://ecsa-7.sciforum.net/>.

Published: 15 November 2020

Abstract: This paper proposes a new readout method for a sensor to detect a minute variations into the capacitance. A sensor is based on the weakly coupled electrical resonators that use an amplitude ratio (AR) as an output signal. A new readout scheme with a relatively higher output sensitivity is proposed to measure the relative changes into the input capacitor. A mathematical model is derived to express the readout output as a function of change into the capacitance. To validate the theoretical model, a system is modelled and designed using an industry-standard electronic circuit design environment. A SPICE simulation results are presented for a wide range of design parameters, such as varying coupling factors between the two electrical resonators. Sensitivity comparison between the existing and the proposed AR readout is presented to show the effectiveness of the method of detection proposed in this work.

Keywords: High-precision physical sensor; Coupled resonator sensor; Readout method for capacitance sensor; WCR; Resonator; MEMS; Capacitance-to-Voltage converter; Readout for Capacitive micromachined transducer

1. Introduction

In today's world, an intelligent electronic circuits [1–3] to detect/ measure minute capacitance change form an integral part of many micromachined/MEMS sensors [4–6]. Often the key design requirements of such capacitive readouts are high sensitivity, ultra-high resolution (low noise floor), low power consumption, etc. However, designing and implementing a high-performance capacitive readout to precisely measure the minute variations in to the input capacitance pose various challenges. These include intrinsic and extrinsic noise sources, board-level parasitics, etc. Recently, a capacitance readout method based on the two weakly coupled resonators (WCR) has been used to measure minute variations in a capacitance [2,7]. This research was done in the context of proposing a readout method for capacitance sensors. Our work presents an innovative, and new readout method to measure small capacitance changes into the micromachined/MEMS transducers. A readout method reflects into the higher changes into the output voltage (relatively higher sensitivity) for small incremental changes into the perturbation (capacitance). A readout circuit is called as capacitance-to-amplitude/ amplitude ratio (AR) converter.

2. Mathematical Model

As shown in Figure 1, consider a RLC circuit that is used to form two electrically coupled resonators (CR) to measure changes into the input capacitance. In this circuit, following assumptions are valid: $L_1 = L_2 = L$, $C_1 = C_2 = C$ and $R_1 = R_2 = R$. This establishes a symmetry in a circuit. A coupling factor between the two individual RLC circuits is modelled as $\kappa = C/C_c$. A change into the input

capacitance is ΔC . The normalized value of the capacitance change (in the form of a perturbation) is expressed as $\delta = \Delta C/C$. Condition for a coupling is given as $C_c \gg C$, indicating two resonant modes can be reasonably distinguished into the output frequency response. The quantities $V_1(t)$ and $V_2(t)$ are input voltages and quantities $I_1(t)$ and $I_2(t)$ are the output loop currents.

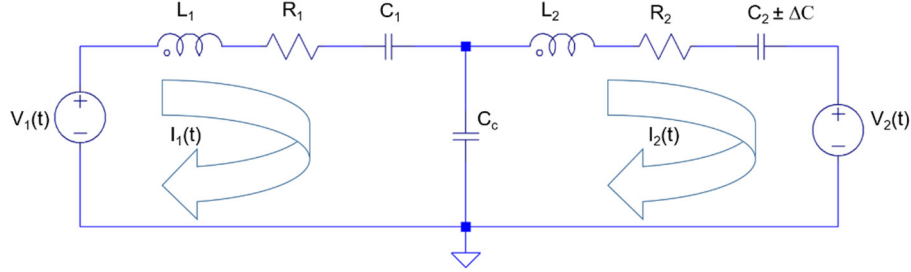


Figure 1. A circuit level schematic representation of a RLC readout.

Assuming no damping in the system, i.e., $R = 0$, a set of governing differential equations are represented as

$$L\ddot{q}_1(t) + \frac{1}{C}q_1(t) + \frac{1}{C_c}[q_1(t) - q_2(t)] = V_1(t) \quad (1)$$

$$L\ddot{q}_2(t) + \frac{1}{C \pm \Delta C}q_2(t) + \frac{1}{C_c}[q_2(t) - q_1(t)] = V_2(t) \quad (2)$$

It is assumed that system is driven with only one voltage source, i.e. $V_1(s) \neq 0$, and $V_2(s) = 0$. Applying Laplace Transform to Equations (1) and (2) yield the following:

$$\left(Ls^2 + \frac{1}{C} + \frac{1}{C_c} \right) Q_1(s) - \frac{1}{C_c} Q_2(s) = V_1(s) \quad (3)$$

$$\left(Ls^2 + \frac{1}{C \pm \Delta C} + \frac{1}{C_c} \right) Q_2(s) - \frac{1}{C_c} Q_1(s) = 0 \quad (4)$$

Solving further one can obtain the transfer functions as

$$H_1(j\omega) = \frac{Q_1(j\omega)}{V_1(j\omega)} = \frac{-L\omega^2 + \frac{1}{C \pm \Delta C} + \frac{1}{C}}{L^2\omega^4 - \left(\frac{L}{C} + \frac{2L}{Cc} + \frac{L}{C \pm \Delta C} \right)\omega^2 + \alpha} \quad (5)$$

$$H_2(j\omega) = \frac{Q_2(j\omega)}{V_1(j\omega)} = \frac{\frac{1}{Cc}}{L^2\omega^4 - \left(\frac{L}{C} + \frac{2L}{Cc} + \frac{L}{C \pm \Delta C} \right)\omega^2 + \alpha} \quad (6)$$

$$\text{Here, } \alpha = \left(\frac{1}{C^2 + CC_c} + \frac{1}{CC_c + C_c \Delta C} + \frac{1}{CC_c} \right).$$

The denominator in (5) and (6) is the characteristic equation which provide the roots. In other words, the roots or eigen-frequencies, ω_i^2 ($i = 1, 2$) as a function of ΔC are obtained as follows:

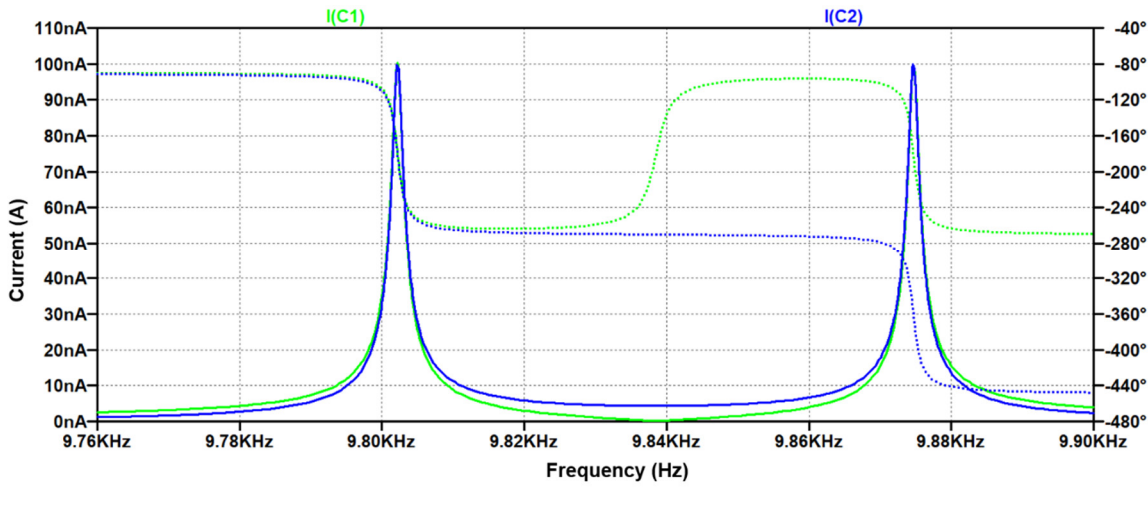
$$\omega_i^2 = \frac{\left(\frac{L}{C} + \frac{2L}{Cc} + \frac{L}{C \pm \Delta C} \right) \pm \sqrt{\left(\frac{L}{C} + \frac{2L}{Cc} + \frac{L}{C \pm \Delta C} \right)^2 - 4L^2\alpha}}{2L^2} \quad (7)$$

Using (7) in (5) and (6), and taking the ratio of $H_1(j\omega)$ and $H_2(j\omega)$, i.e., $\frac{Q_1(j\omega_i)}{Q_2(j\omega_i)}$ provides the charge output amplitude ratio (AR). The amplitude ratio, AR_i ($i = 1, 2$) as a function of ΔC then is obtained as

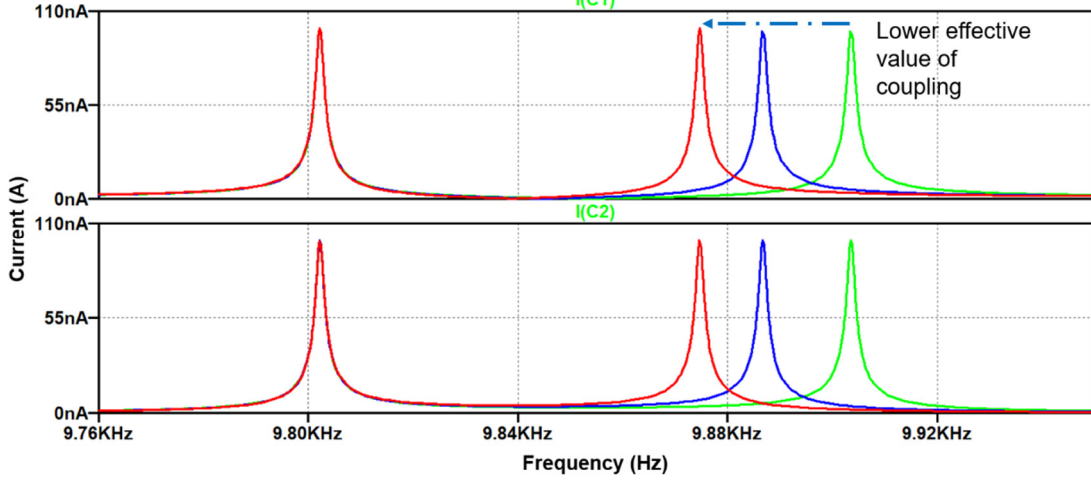
$$\frac{Q_1(j\omega_i)}{Q_2(j\omega_i)} = \frac{-L \left(\frac{L}{C} + \frac{2L}{C_c} + \frac{L}{C \pm \Delta C} \right) \pm \sqrt{\left(\frac{L}{C} + \frac{2L}{C_c} + \frac{L}{C \pm \Delta C} \right)^2 - 4L^2 \alpha}}{2L^2} + \frac{1}{C \pm \Delta C} + \frac{1}{C} \quad (8)$$

3. SPICE Modeling and Results

Figure 2a shows a resulting plots of the output loop currents of a RLC readout circuit model seen in Figure 1. A fixed value of the coupling capacitor C_c is used for the simulation. Note that equal output amplitudes of the loop currents represent initial symmetry of the system. Figure 2b presents similar plots of the output loop currents for varying values of the coupling capacitor C_c . Higher effective values of C_c leads to the lower effective value of a coupling between the two resonant circuits. A relatively weaker coupling is reflected by the closed-spacing of the mode-frequencies as seen from the plots.



(a)



(b)

Figure 2. (a) Frequency response of a coupled RLC system for a fixed value of a coupling, magnitude (left) and phase (right); (b) Frequency response of a coupled RLC system for variants of effective coupling. Lower coupling leads to closely-spaced mode frequencies.

Figure 3 presents a frequency response of a coupled RLC for a fixed value of a coupling and variants of a perturbations used. As can be observed, upon applying a minute changes (ΔC) into the input capacitor, C_2 (refer Figure 1), variations in both the resonant mode frequencies and mode amplitudes of each resonators are observed.

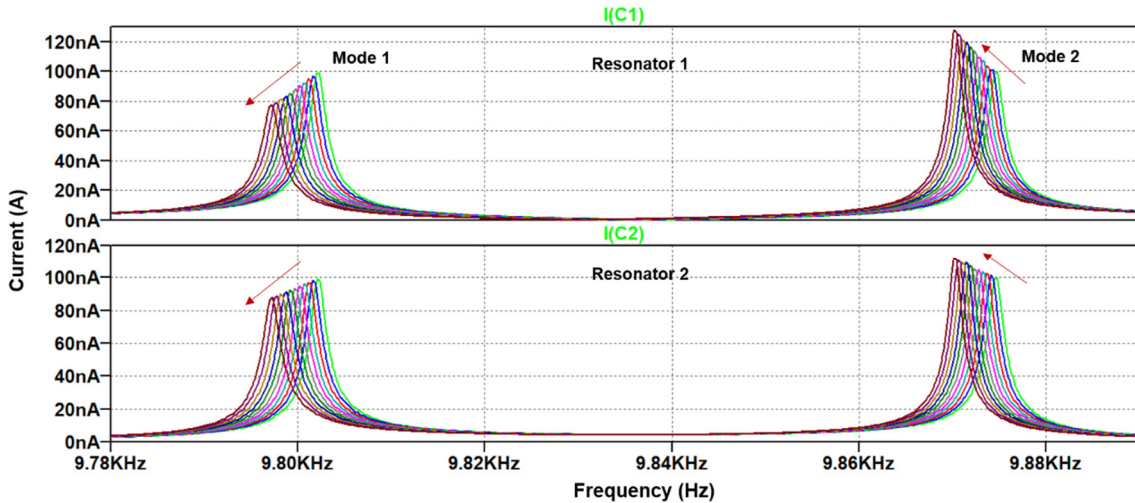


Figure 3. Frequency response of a coupled RLC capacitance sensor system. Top plot shows response of resonator 1 and bottom plot shows response of resonator 2. Direction of arrow indicates a variation trend of the resonant peak of the j^{th} ($j = 1, 2$) resonator at the i^{th} ($i = 1, 2$) mode of the frequency response.

4. A New Readout Method (Measure at ω_0 Instead of ω_i)

A conventional method of sensing the capacitance perturbation is existent in the literature [2]. Such method relies on the fact that mode-frequencies and amplitude ratio vary as a function of ΔC (Equations (7) and (8)).

AR method of sensing is being pursued owing to the relatively higher sensitivity to the input perturbations into the weakly coupled resonant system. In our work, we propose a new method of sensing in which amplitude/s and/or AR of the j^{th} resonator ($j = 1, 2$) at the i^{th} mode ($i = 1, 2$) is recorded at the initial resonant mode-frequency, ω_0 (instead of ω_i) when perturbation is applied into the system. This can be illustrated from Figure 4 that presents a frequency response of the j^{th} resonator ($j = 1, 2$) at the first resonant mode. As seen, an arrow indicates an amplitude change of the j^{th} resonator ($j = 1, 2$) when ΔC is applied into the system and this is the conventional output of a readout. We instead propose to sense the amplitude shifts at the resonance for each applied values of ΔC . This is indicated by dots forming a downward line in Figure 4. Similar readout approach can be utilized with a frequency response of the j^{th} resonator ($j = 1, 2$) at the second resonant mode.

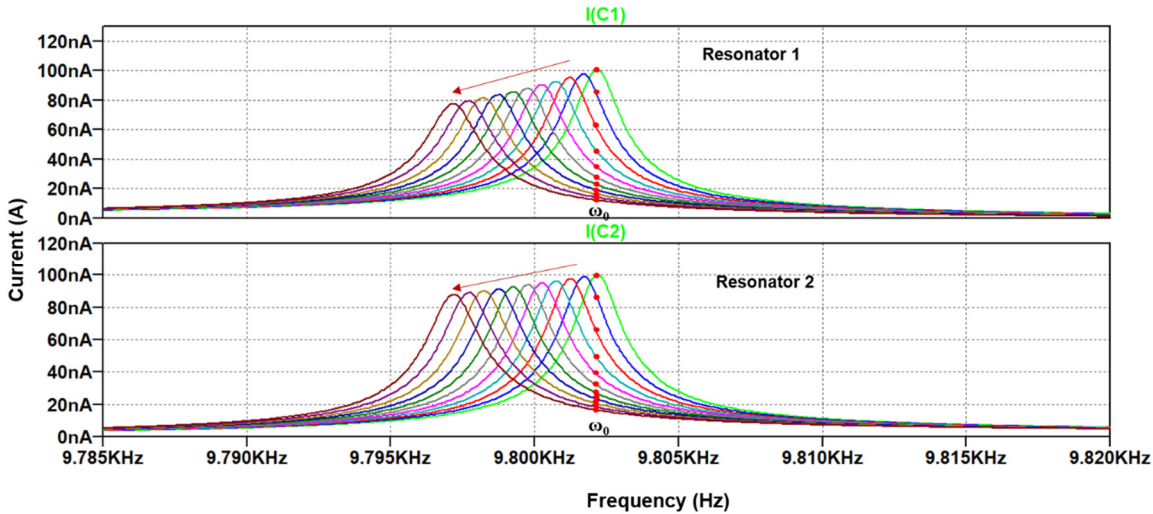


Figure 4. Frequency response of a coupled RLC capacitance readout system. Response of resonator 1 (top) and response of resonator 2 (bottom). Direction of dotted line indicates measuring a proposed variation trend of the resonant peak of the j^{th} ($j = 1, 2$) resonator at the i^{th} ($i = 1, 2$) mode of the frequency response. Shown here is the output response of the j^{th} ($j = 1, 2$) resonator at the first mode of a coupled RLC resonant capacitance readout.

Figure 5a shows output amplitude response of a RLC coupled resonators. It shows how amplitudes of the j^{th} resonator ($j = 1, 2$) varies as a function of % variation in δ . In the same plot, it also shows how amplitudes of the j^{th} resonator ($j = 1, 2$) varies as a function of % variation in the δ if proposed method of readout is used. Clearly, a linear (up to certain range) and higher output is available with the new method of readout. Figure 5b provides a final readout in terms of AR of the system. Two AR readout methods are seen in the plot. A proposed AR readout method shows higher changes into the output for small incremental changes into the capacitance.

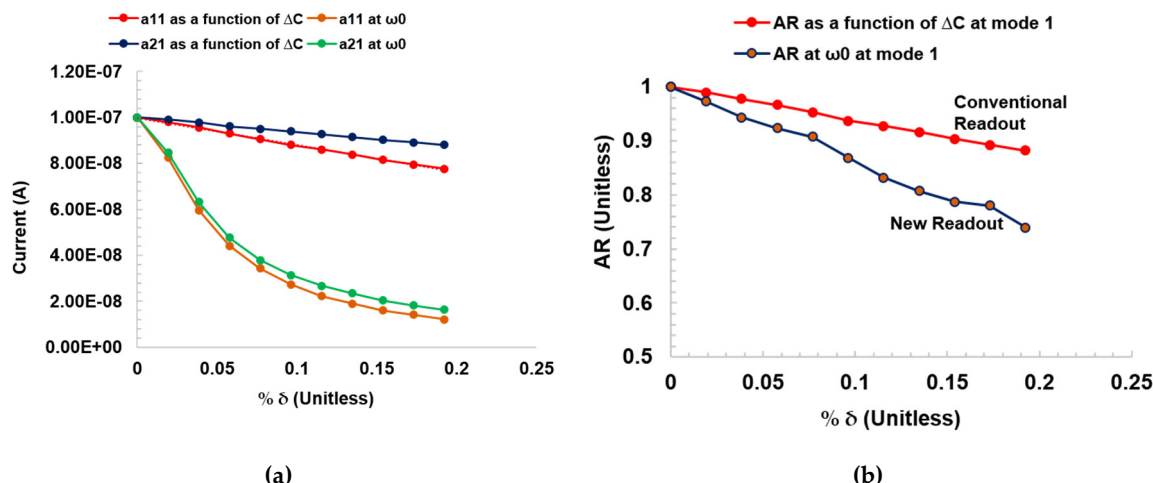


Figure 5. Output response of a coupled RLC capacitance readout circuit. (a) Output current amplitude vs ΔC or δ . Label a_{11} is amplitude of resonator 1 at mode 1, a_{21} is amplitude of resonator 2 at mode 1 (b) Amplitude ratio (AR) readout of RLC coupled resonator circuit. ω_0 is the initial readout resonant frequency at mode 1.

5. Conclusions

A new readout method using an electrically coupled resonator circuits is proposed. Such readout circuit when interfaced with the micromachined transducer can be effective for the enhanced sensitivity output. Same concept of the readout can be extended to the MEMS resonators and other inertial sensors, where overall system can benefit from the high quality factor of the MEMS

transducers/sensors. Extended work should involve improving the linearity in the output of the proposed readout method.

Funding: This research received no external funding.

Conflicts of Interest: The authors declare no conflict of interest.

References

1. Pérez Sanjurjo, J.; Prefasi, E.; Buffa, C.; Gaggl, R. A Capacitance-To-Digital Converter for MEMS Sensors for Smart Applications. *Sensors* **2017**, *17*, 1312.
2. Hafizi-Moori, S.; Cretu, E. Weakly-coupled resonators in capacitive readout circuits. *IEEE Trans. Circ. Syst. I Regul. Pap.* **2015**, *62*, 337–346.
3. Qiao, Z.; Boom, B.A.; Annema, A.J.; Wiegerink, R.J.; Nauta, B. On frequency-based interface circuits for capacitive MEMS accelerometers. *Micromachines* **2018**, *9*, 488.
4. Utz, A.; Walk, C.; Stanitzki, A.; Mokhtari, M.; Kraft, M.; Kokozinski, R. A High-Precision and High-Bandwidth MEMS-Based Capacitive Accelerometer. *IEEE Sens. J.* **2018**, *18*, 6533–6539.
5. Kose, T.; Terzioglu, Y.; Azgin, K.; Akin, T. A single-mass self-resonating closed-loop capacitive MEMS accelerometer. In Proceedings of the IEEE Sensors, Orlando, FL, USA, 30 October–3 November 2017.
6. Nazemi, H.; Balasingam, J.A.; Swaminathan, S.; Ambrose, K.; Nathani, M.U.; Ahmadi, T. Mass sensors based on capacitive and piezoelectric micromachined ultrasonic transducers—CMUT and PMUT. *Sensors* **2020**, *20*, 2010.
7. Hafizi-Moori, S.; Cretu, E. Reducing measurement error in capacitive readout circuits based on weakly coupled resonators. *IEEE Sens. J.* **2017**, *17*, 735–744.

Publisher's Note: MDPI stays neutral with regard to jurisdictional claims in published maps and institutional affiliations.



© 2020 by the authors. Submitted for possible open access publication under the terms and conditions of the Creative Commons Attribution (CC BY) license (<http://creativecommons.org/licenses/by/4.0/>).